Ionic Polymer-Metal Composite Enabled Robotic Manta Ray

Zheng Chen*, Tae I. Um, and Hilary Bart-Smith

Bio Inspired Engineering Research Laboratory
Department of Mechanical & Aerospace Engineering
University of Virginia, Charlottesville, VA 22904, USA.

ABSTRACT

The manta ray, *Manta birostris*, demonstrates excellent swimming capabilities; generating highly efficient thrust via flapping of dorsally flattened pectoral fins. In this paper, we present an underwater robot that mimics the swimming behavior of the manta ray. An assembly-based fabrication method is developed to create the artificial pectoral fins, which are capable of generating oscillatory with a large twisting angle between leading and trailing edges. Ionic polymer-metal composite (IPMC) actuators are used as artificial muscles in the fin. Each fin consists of four IPMC beams bonded with a compliant poly(dimethylsiloxane) (PDMS) membrane. By controlling each individual IPMC strips, we are able to generate complex flapping motions. The fin is characterized in terms of tip deflection, tip blocking force, twist angle, and power consumption. Based on the characteristics of the artificial pectoral fin, a small size and free-swimming robotic manta ray is developed. The robot consists of two artificial pectoral fins, a rigid body, and an on-board control unit with a lithium ion rechargeable battery. Experimental results show that the robot swam at a speed of up to 0.055 body length per second (BL/sec).

Keywords: Ionic Polymer-Metal Composites, Biomimetic Actuation, Robotic Manta Ray

1. INTRODUCTION

The manta ray (*Manta birostris*) is the largest species of rays. They are a flat-bodied cartilaginous fish and have the largest brain-to-body ratio of members within the elasmobranchii subclass, which includes sharks, rays and skates.[1] The manta ray can utilize two pectoral fins to perform high efficiency swimming and maneuvering by generating 3 dimensional (3D) kinematic motions.[2] Many efforts have been directed towards building a bio-inspired fin structure to mimic the swimming behavior of the manta ray. Moored *et al.*[3] developed an large amplitude and oscillatory-type artificial pectoral fin. The artificial fin structure is composed of some plates, which are embedded in a planform shaped elastomer fin, and actuated by a linear electric motor. It is capable of generating large deflections under significant loads. However, it can only generate oscillation motion. Moored *et al.*[4] developed a tensegrity structure that acts as the structural foundation of an artificial pectoral fin for a robotic manta ray. The artificial fin structure is composed of cable-routed aluminum rods and is actuated by multiple linear electric motors, which can generate 3D kinematic motions under high loads. Due to size limitations in manufacturing these active tensegrity structures, alternative solutions are being investigated to produce a small scale robot (on the order of 5-10 cm), which has promising applications in underwater environmental monitoring.[5] A bio-inspired actuation material, which is lightweight, compliant, resilient, and capable of being fabricated into any arbitrary shape, is desirable in making a power efficient and small scale robotic manta ray.

Electroactive polymers (EAPs), sometimes referred to as artificial muscles, are able to generate large deflections under electrical stimulus.[6] Ionic polymer metal composites (IPMCs) are an important category of EAPs.[7] Since IPMCs can work well in a sodium salt water environment, they show promise as actuators for underwater robots in ocean applications. An IPMC consists of one ion exchange membrane, such as Nafion, coated with two thin metal electrodes.[8] When the IPMC is hydrated, the positive ions in the Nafion polymer, such as sodium and calcium ions, can move freely, whereas the negative ions are bonded on the carbon chain. Application of an

Further author information: (Send correspondence to Zheng Chen)
Z. Chen: zc7u@virginia.edu, T. Um: tiu2f@virginia.edu, H. Bart-Smith: hb8h@virginia.edu

Electroactive Polymer Actuators and Devices (EAPAD) 2011, edited by Yoseph Bar-Cohen, Federico Carpi,
Proc. of SPIE Vol. 7976, 797637 · © 2011 SPIE · CCC code: 0277-786X/11/$18 · doi: 10.1117/12.880452

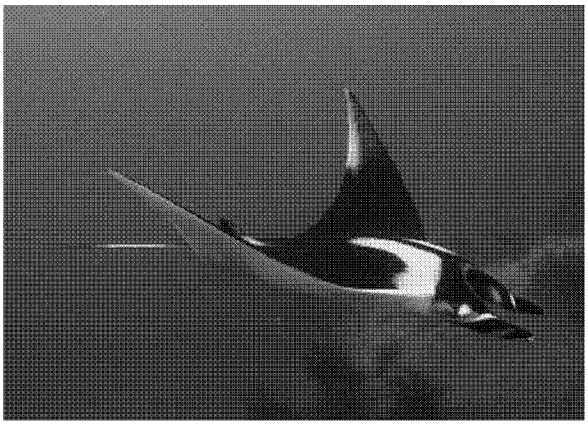

Figure 1. Bio-inspiration: manta ray (courtesy of www.elasmodiver.com).

electric field causes the hydrated cation to move the cathode side with the negative ions fixed in position. This ion movement introduces swelling in the polymer close to the cathode side, which leads to the bending motion of IPMC. An IPMC actuator has been used as the caudal fin of a bio-inspired robotic fish.[9] The propulsive fin mimics the bending motion observed in many fish species. In order to achieve more complex 3D kinematics, Chen and Tan[10] used lithographic patterning technology to design an artificial pectoral fin. This fabrication process has proved to be good for fabricating fins with micron scale feature. However, the process includes lithography patterning, plasma etching, and PVD deposition, all which are expensive and time consuming. Anton *et al* developed pectoral fins for ray-like underwater robot by assembling separated IPMC beams with a latex foil.[11] However, their robot design failed to achieve any visible rectilinear motion. The mobility of the robot was further limited by a tether.

In this study, a small size and free swimming robotic manta ray propelled by two IPMC artificial pectoral fins has been successfully developed. An assembly-based fabrication technique has been developed to integrate the IPMC actuators into an artificial pectoral fin design. The fin is fabricated by bonding four IPMC beams with a 190 μm thick membrane of polydimethylsiloxane (PDMS). The overall shape of the fin mimics that of biology. Each IPMC beam is controlled individually to produce bending motions with different amplitude and phase, leading to complex kinematic motions similar to those observed in nature. In the characterization of the pectoral fin, the fin is actuated to generate oscillation and undulatory motions by controlling the phase delay of the voltage signals applied to the IPMCs. The fin is characterized by the key factors in the function of the robot: tip deflection, tip blocking force, twisting angle, and power consumption. Based on the experiments conducted, the pectoral fin is able to generate up to 25% tip deflection, 1 gram tip blocking force in oscillating motion, and 15° twisting angle in undulatory motion. The measured power consumption of one fin is less than 0.5 Watts. It has been verified that the pectoral fin is capable of generating oscillation and undulatory motions with low power consumption. In the robot design, a plastic frame with gold electrodes is fabricated as the body of the robot. A light and compact on-board control unit with a lithium ion polymer battery has been developed for generating control signals to two pectoral fins. The width, length, and mass of the robot are 18 cm, 8 cm, and 55 grams, respectively. Experimental results show that the robot is able to swim at the speed up to 0.055 BL/sec. This is the first demonstration of a free-swimming robotic manta ray propelled by IPMC artificial muscles. Since the pectoral fin can be easily fabricated in different shapes and dimensions, this research provides a platform to investigate the propulsion mechanisms of different types of rays.

The rest of this paper is organized in the following manner. Artificial pectoral fin fabrication is described in Section 2. Characterization of the fin is discussed in Section 3. The design of the robotic manta ray is shown in Section 4. The free swimming testing of the robot is discussed in Section 5 where snap shot of swimming robot has shown. The conclusion and future work are discussed in Section 6.

2. FABRICATION OF ARTIFICIAL PECTORAL FIN

The proposed robotic manta ray must be able to generate complex kinematic motions, such as the oscillatory and undulatory motions observed in nature, while under hydrodynamic loads. In this paper, an artificial pectoral fin is fabricated by combining IPMC actuators with a PDMS elastomer template to create a predefined planform shape. The design of pectoral fin is shown in Fig. 2. The shape of the outline of the fin is similar to that of the biological manta ray. P_1, P_2, P_3, and P_4 are 10 mm wide IPMC beams with 30 mm, 50 mm, 70 mm, and 50 mm lengths, respectively.

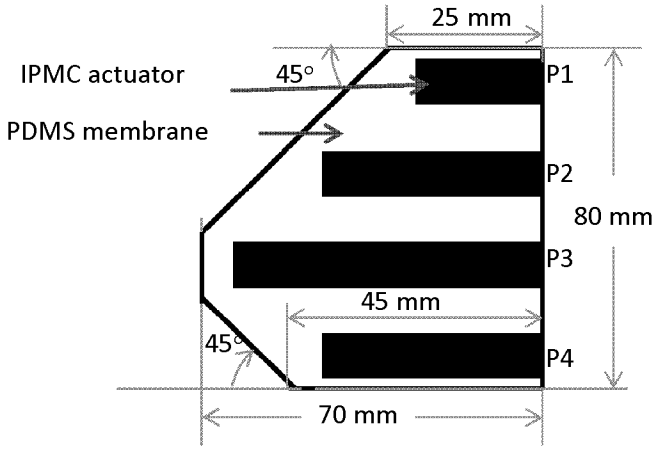

Figure 2. Artificial pectoral fin design.

The first step in creating the artificial pectoral fin is to fabricate the IPMC actuators. Many groups have developed different IPMC fabrication processes for various purposes.[7,12–14] In our fabrication method, we followed most of the procedure outlined by K. Kim and M. Shahinpoor[12] but added a multiple platinum plating process to reduce the surface resistance of the electrodes.[15] After the IPMC has been fabricated, the next step is to bond this with a PDMS elastomer membrane. This membrane will create the planform shape of the artificial pectoral fin. The PDMS bonding process is shown in Fig 3. First, we make two Delrin polymer (McMaster) molds using a CNC rapid milling machine (MDX-650, Roland). Each mold has two concaved areas to house PDMS passive membrane and IPMC actuator in the molding process. The thickness of PDMS membrane is 190 μm and thickness of IPMC is 280 μm. Second, we cut IPMC into four rectangle strips P_1, P_2, P_3, and P_4 (shown in Fig. 2). Third, we clamp IPMCs and PDMS gel (Ecoflex 0030, Smooth-on Inc.) with the mold and cure the PDMS at room temperature for 3 hours. Finally, we remove the mold and get the IPMC/PDMS artificial pectoral fin which is shown in Fig. 4.

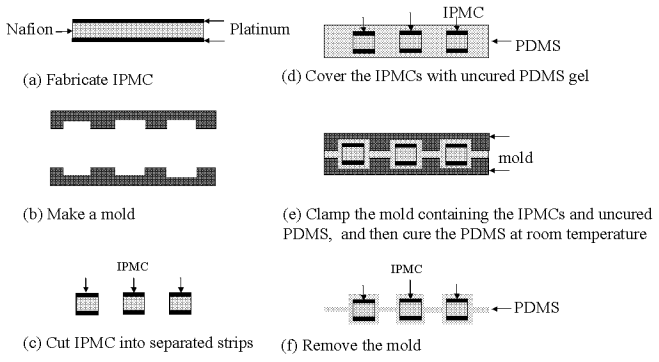

Figure 3. Fabrication process.

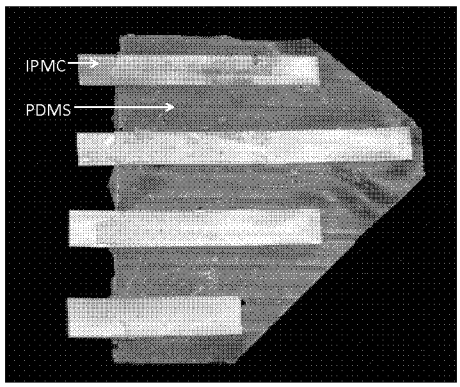

Figure 4. IPMC/PDMS artificial pectoral fin.

3. CHARACTERIZATION OF ARTIFICIAL PECTORAL FIN

The pectoral fin is characterized in terms of tip deflection, tip force, twist angle, and power consumption. These characteristics are useful in providing comparison data in the design of the bio-inspired robot. To characterize the actuating response of the pectoral fin, five testing points (A, B, C, D, E) are defined on the actuator (shown in Fig. 5).

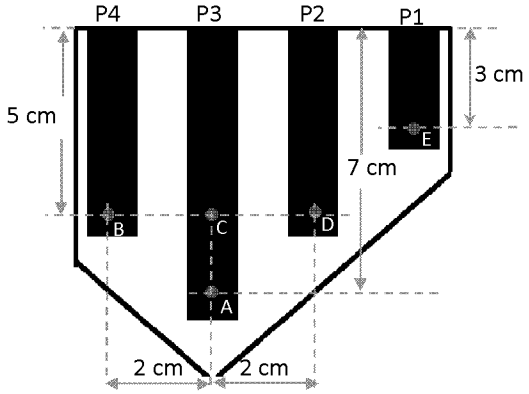

Figure 5. Testing points of the pectoral fin.

3.1 Tip deflection measurement

The pectoral fin is actuated in a transparent tank containing water. A laser sensor (OADM 20I6441/S14F, Baumer Electric) is fixed outside of the tank to measure the bending displacement at point A. The tip deflection is normalized by dividing the bending displacement by the length at point A. Fig. 6 shows the tip deflection when a square wave actuation voltage (0.3 Hz, 3.3 V) is applied to all the IPMCs. It shows a peak-to-peak deflection of 25% of the spanwise dimension. One can achieve a larger deflection by applying a higher actuation voltage. There is a limit to the size of voltage applied across the IPMC–anything greater than 6 V risks dielectric breakdown through the IPMC.

To capture the Bode plot of the actuation dynamics of the fin, a series of sinusoidal actuation signals with an amplitude of 3 V and frequencies ranging from 0.1 Hz to 2 Hz are applied to the IPMCs. The bending displacement at Point A and actuation voltage are measured. The magnitude and phase shift of the displacement over the actuation voltage are calculated. The Bode plot (Fig. 7) demonstrates that the actuation dynamics of the pectoral fin behaves as a low-pass filter with about 0.4 Hz cut-off frequency. This is to be expected as the ions in the IPMC cannot move very rapidly[16] and the hydrodynamic forces acting on the fin damp the high frequency vibration.[17]

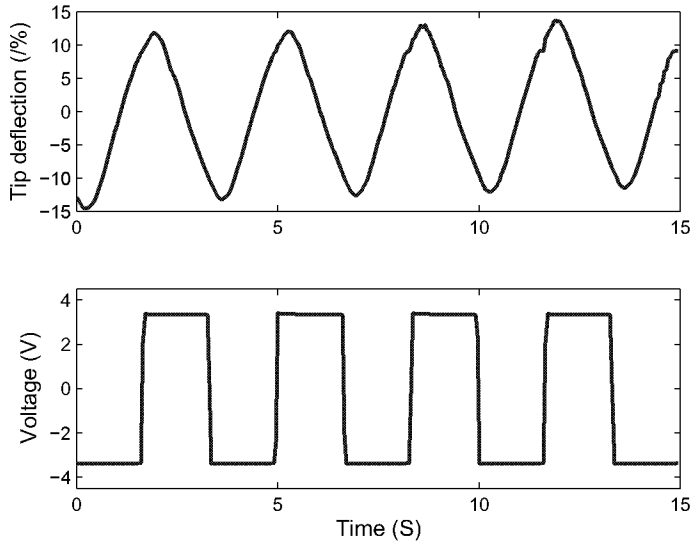

Figure 6. Tip deflection at point A under a square wave actuation voltage (0.3 Hz, 3.3 V).

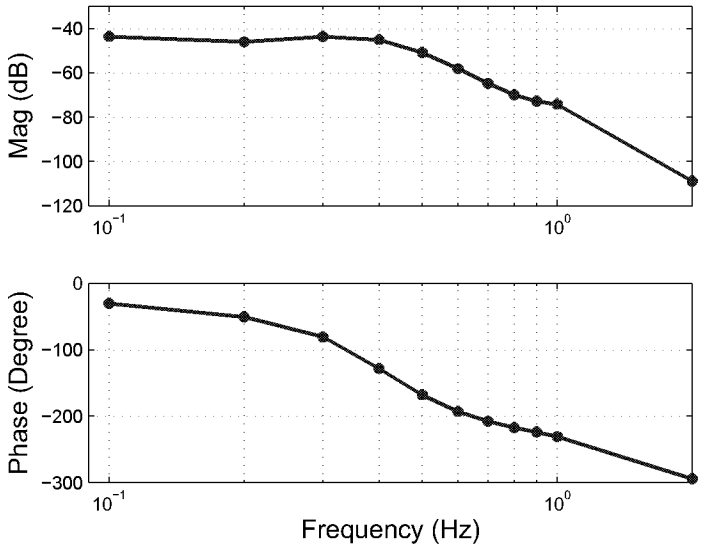

Figure 7. Bode plot of the actuation dynamics of the pectoral fin.

3.2 Tip force measurement

To characterize the tip force, a load cell (GS0-10, Transducer Techniques) is used to measure the tip blocking force at point A, B, D, and E (See Fig. 5). The measurement range of the load cell is from 0 to 10 grams. The calibration error of the load cell, including hysteresis, nonlinearity, and non-repeatability, is 3 milligrams. The measurements are taken in air and are recorded in four separate experiments. In each experiment, a 4 V step voltage is applied to all the IPMCs. Fig. 8 shows the tip force response at Point A, where steady-state force F_s and rising time T_r are defined. The tip blocking force on each IPMC has been measured twice. Table 3.2 shows the mean values of F_s and T_s and their variations.

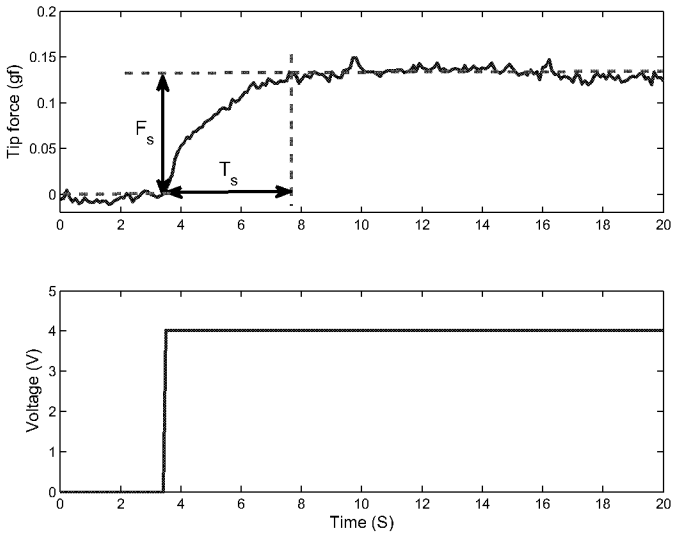

Figure 8. Tip force measurement at point A under a 4 V step actuation voltage.

Table 1. Tip force measurement.

	At Point A	At Point C	At Point D	At Point E
$\overline{F_s}$ (gf)	0.16	0.34	0.49	0.67
$\frac{\Delta F_s}{\overline{F_s}}$	±19%	±5.5%	±4.7%	±7.4%
$\overline{T_r}$ (S)	4.05	7.95	8.65	9.10
$\frac{\Delta T_r}{\overline{T_r}}$	±1.2%	±3.1%	±1.0%	2.0%

3.3 Power consumption measurement

For applications like an untethered bio-inspired robot, key questions regarding power consumption and how to optimally manage power consumption must be addressed. In this section, we study the power consumption under a square wave input. The power consumed by IPMCs is calculated by:

$$P = \frac{1}{T}\int_0^T i(t)v(t)dt, \tag{1}$$

where $i(t)$ and $v(t)$ are measured actuation current and voltage, respectively, and T is the period of the actuation signal. A 3.3 V and 0.22 Hz square wave voltage is applied to all the IPMCs of one pectoral fin, which is fixed in a water tank. Fig. 9 shows the actuation voltage and current. To study the relation between the power

consumption and frequency, a series of square wave actuation signals with an amplitude of 3.3 V and frequencies ranging from 0.22 Hz to 0.58 Hz are applied to the fin. Fig. 10 shows the power consumed versus frequency graph. It demonstrates that they are positively related and the power consumption at the cut-off frequency 0.4 Hz is 0.483 W.

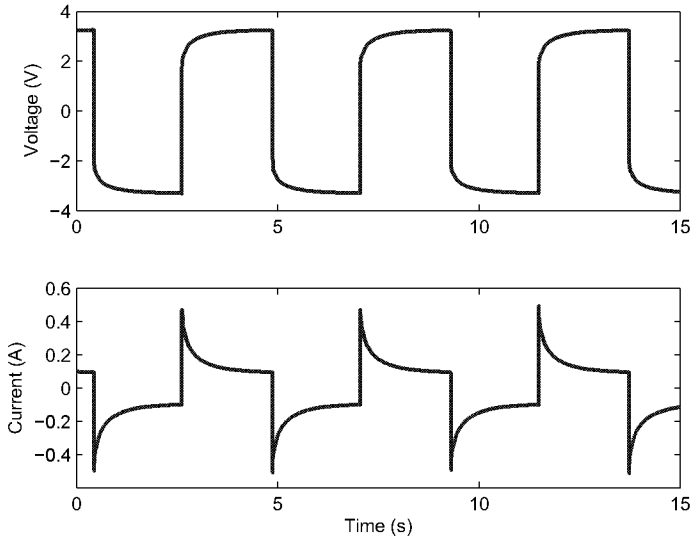

Figure 9. Actuation current measurement.

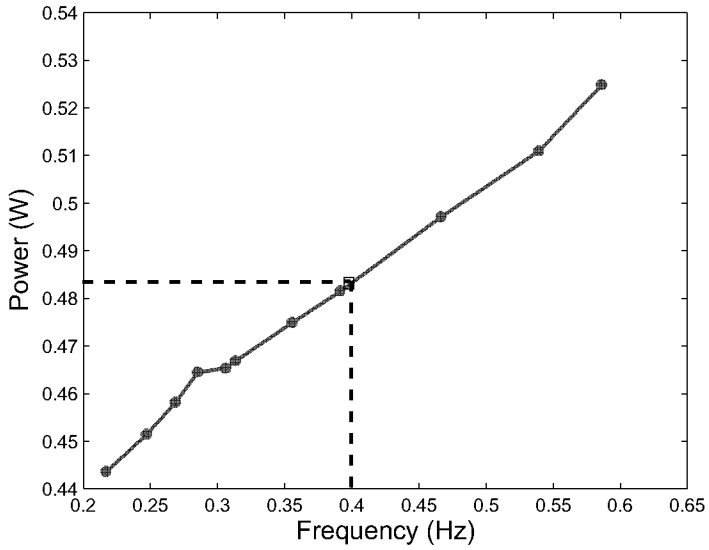

Figure 10. Power consumption versus frequency.

3.4 Characterization of the fin's 3D kinematics

In order to characterization of the fin's 3D kinematics, definition of twist angle is given in Fig. 11, where points B, C, and D are defined in Fig. 5. Three laser sensors (OADM 20I6441/S14F, Baumer Electric) are used to measure

the bending displacements d_1, d_2, and d_3 at the point B, C, D, respectively. The twist angles are calculated by

$$\alpha_1 = \arctan \frac{d_2 - d_1}{BC}, \ \alpha_2 = \arctan \frac{d_3 - d_2}{CD}, \tag{2}$$

where $BC = CD = 20$ mm.

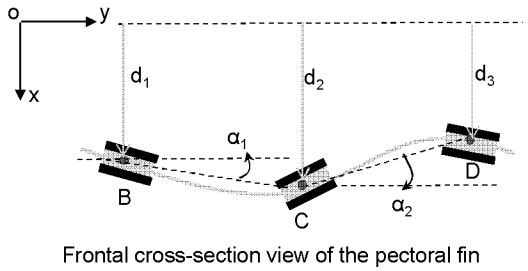

Figure 11. Definition of twist angles.

Four sinusoidal voltage signals (S_1, S_2, S_3, and S_4) are generated via Labview (National Instruments), amplified by power amplifiers, and applied to the IPMC actuators P_1, P_2, P_3, and P_4 (shown in Fig. 2), respectively. All signals have the same input voltage of 6 V but varying phases. The phase ϕ in this paper is defined as the following. If $\phi = \mathrm{A}^\circ$, then following Fig. 3, P_i leads P_{i+1} by A°, where $i = 1, 2, 3$. As mentioned earlier, IPMC actuators are used to generate thrust in underwater vehicles. Hence the kinematics are quantified in water. The fin is placed in a water tank and the laser sensors are fixed outside of the tank. Fig. 12 shows the experimental results at $\phi = 60^\circ$. The upper figure shows the bending displacement d_1, d_2 and d_3, which clearly shows the phase delay between the bending motion of the IPMC P_1, P_2, and P_3. The lower figure shows the calculated twist angles α_1 and α_2. These results demonstrate that one can control the twist motion by manipulating ϕ. The maximum twist angle is 15.5°, which is similar to the angle generated by the pectoral fin in Chen and Tan.[10]

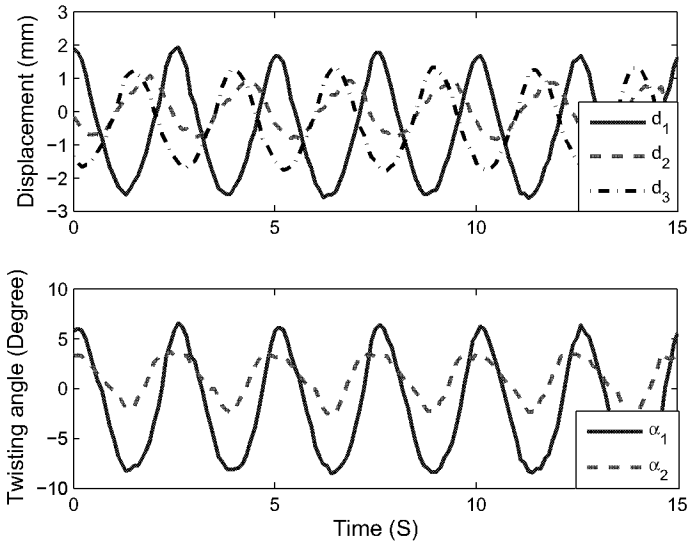

Figure 12. Bending displacements and twist angles under the input signals (0.4 Hz, 6 V, and 60° phase)

To demonstrate the dependence of twist angle on frequency and phase, we conducted 16 trials by changing the frequency (0.1 Hz, 0.2 Hz, 0.3 Hz, and 0.4 Hz) and phase (30° 45°, 60°, and 90°). In each trial, the peak to

peak twist angles, α_{1max} and α_{2max}, were measured. Fig. 13 shows the peak to peak twist angle versus different frequency and phase. It shows that $\alpha_1 > \alpha_2$. It may be due to the fact that the actuation of P4 constrains the twist angle α_2. The maximum twist angle is observed when the actuation frequency is 0.4 Hz and the phase is 60^o. Because the motions of IPMCs are constrained by the soft PDMS membrane, the dynamics of the twist angle is complex.

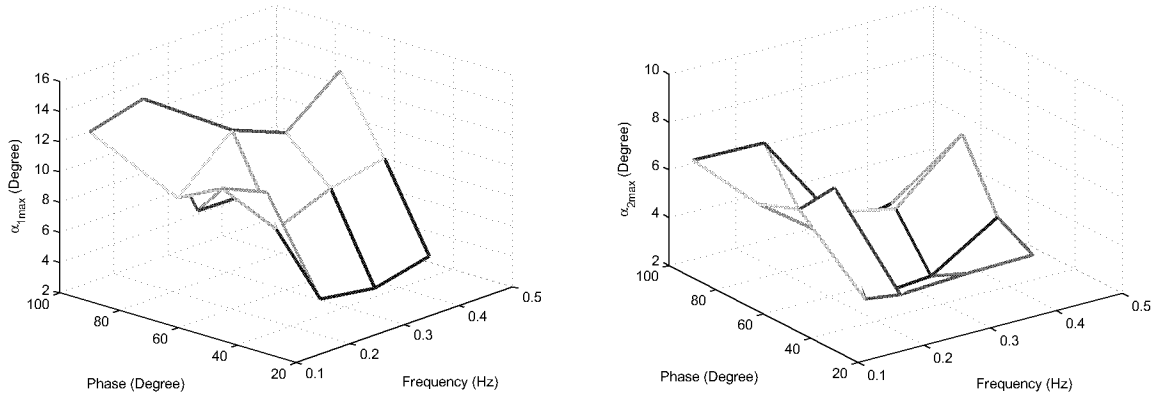

(a) (b)

Figure 13. Peak to peak twist angle versus different frequency and phase. (a) α_{1max}; (b) α_{2max}.

4. DESIGN OF FREE SWIMMING ROBOTIC MANTA RAY

An IPMC enabled ray-like underwater robot was first developed by Anton *et al.*[11] They used 16 IPMC beams connected with latex foil to generate an undulatory wave in the chordwise direction, which enabled rectilinear swimming in the robot. However, this design was constrained by many tethers. The actuators were controlled by a PC computer and powered by several heavy car batteries. Consequently, the robot was severely limited in its swimming capabilities. In this paper, an IPMC robotic manta ray has been designed that is capable of free swimming. It includes a waterproof on-board control unit, two artificial pectoral fins, and a neutrally buoyant lightweight body.

4.1 On-board circuit and battery

The on-board circuit provides actuation voltage signals to the IPMC actuators in the wing. Fig 14(a) shows the schematic of the circuit. In the first iteration, the circuit is able to generate one signal to all the IPMCs, generating a flapping motion. A 555 timer is used to generate a frequency tunable square wave. The amplitude of the voltage signal, V_p, is controlled by an adjustable voltage regulator. Since the 555 timer can only draw 25 mA current while the peak driving current of IPMCs in two pectoral fins is 1.5 A (shown in Fig. 9), an H-bridge driver is used to draw up to 2 A output peak current. In PCB design, most of the chips are in surface-mount package, which makes the circuit board compact (2.5 cm by 3 cm) and light (25 grams).

A lithium ion battery is chosen as the power source since it is lightweight, rechargeable with high power density, and has previously been successfully implemented in IPMC actuated underwater robots.[18] A rechargeable 7.3 V Lithium Ion Polymer battery (400 mAh, AA Portable Power Corp) is selected for the robot. When the robot is running at 0.4 Hz, the power consumption for operating two pectoral fins is 0.96 W (shown in Fig. 10). Ideally, the robot can swim for 2.7 hours without recharging when the operating frequency is 0.4 Hz. The total mass of the circuit and battery is 28.3 grams. Fig. 14 (b) shows the picture of PCB board and battery.

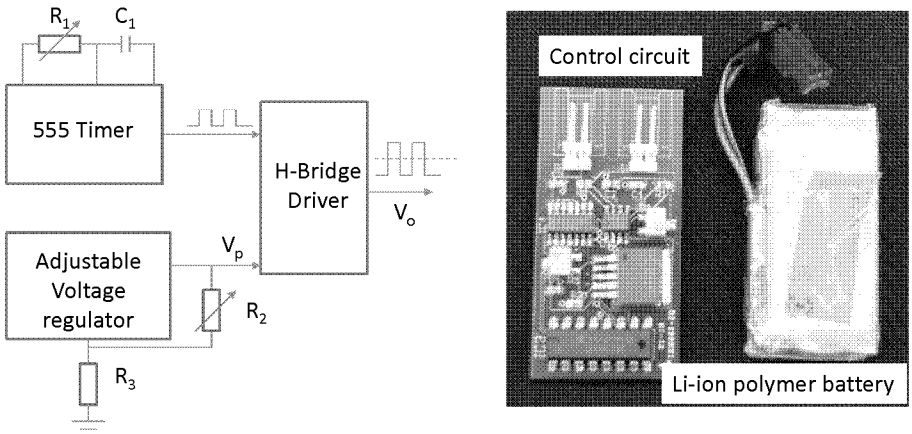

(a) Schematic of circuit board (b) Picture of PCB board and battery

Figure 14. On-board circuit and battery.

4.2 Overall design

Fig. 15 (a) shows the overall shape of the robot. Two acrylic frames with gold electrodes are made to clamp the artificial wings to the body support. Gold electrodes are used to minimize corrosion. An acrylic polymer tail is connected at the end of the robot to aid in stabilizing the body while swimming. Polymer foam is added to make the robot neutrally buoyant. A simple hinged plastic box is used to house the circuit board and battery. Once closed, only two wires leave the box. PDMS is used to seal the housing to ensure water does not invade this compartment. The plastic box is glued on the top of the robot. When the robot is put in water, the cover of the box is above the water level and water cannot leak into the box. Design of the pectoral fins is shown in Fig. 2. The planform shape has been designed to mimic the planform shape of the pectoral fin of a manta ray. The fully assembled robot is 8 cm long (not including the length of the tail), 18 cm wide, 2.5 cm high, and weights 55.3 grams. The free-swimming robot is shown in Fig. 15 (b).

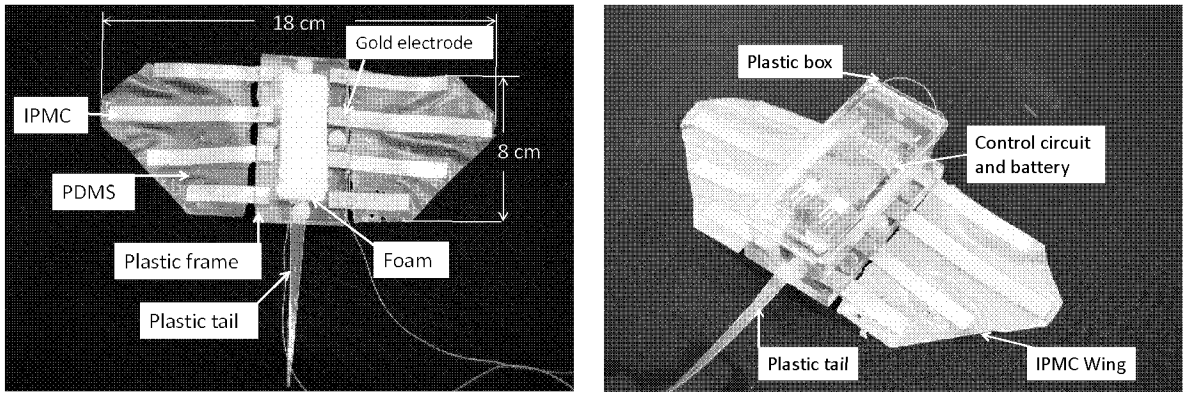

(a) (b)

Figure 15. Robotic manta ray. (a) Without control unit; (b) With control unit.

5. FREE SWIMMING TEST

The robot is tested in a water tank (1.5 m wide, 4.7 m long, and 0.9 m deep). As the first attempt, the operating frequency of the square wave actuation voltage is tuned at 0.4 Hz and the amplitude is set at 3.3 V. A digital video camera (VIXIA HG21, Canon) is used to capture the movies of the swimming robot. Fig. 16 shows six

snap shots of the swimming robot from top view. Each snap shot is taken every 5 second. One can extract the speed of the robot from the movie through the Edge Detection program in the Labview. The swimming speed shown in Fig. 16 is 0.44 cm/sec. Since the body length is 8 cm, one can calculate the speed is 0.055 BL/sec. This is believed to be the first demonstration of an IPMC propelled free-swimming robotic manta ray.

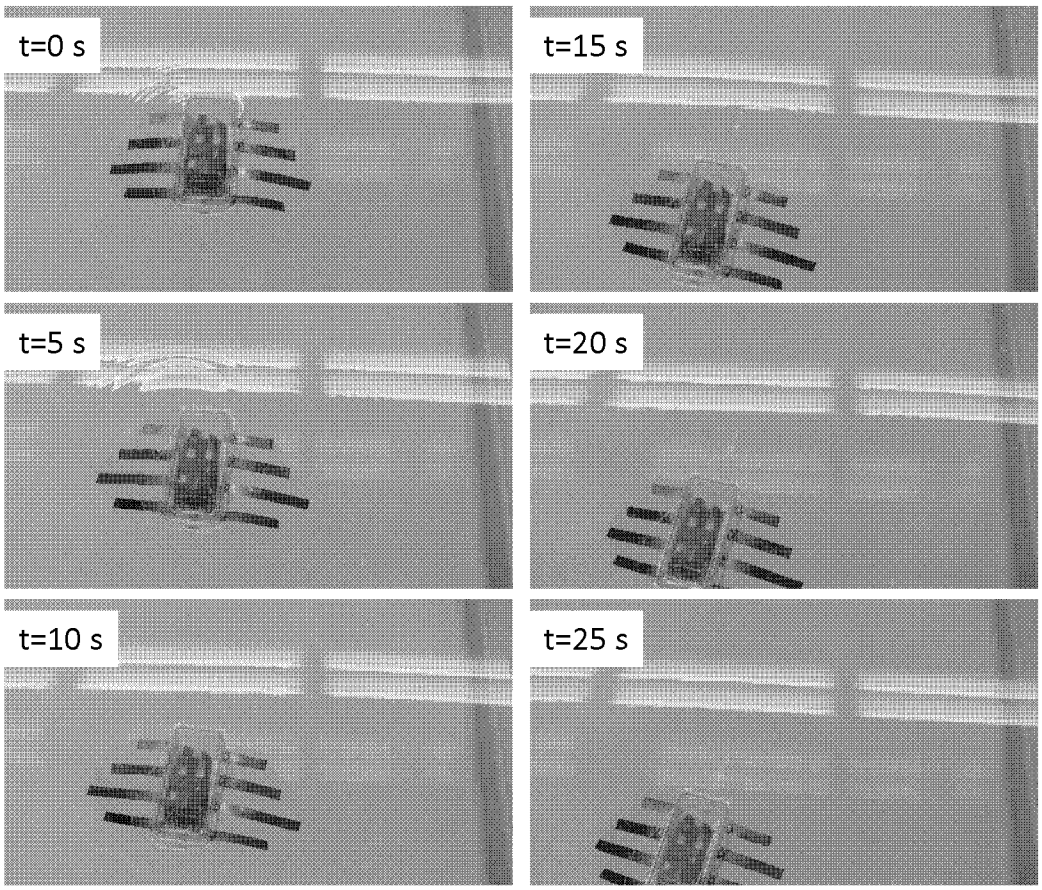

Figure 16. Video 1 Movie of free-swimming robotic manta ray, http://dx.doi.org/10.1117/12.880452.1.

6. CONCLUSIONS AND FUTURE WORK

In this paper, a bio-inspired robotic manta ray propelled by IPMC artificial pectoral fins has been developed. The artificial pectoral fin is fabricated by assembling IPMC actuators with a PDMS elastomer membrane. The fin is characterized in terms of tip deflection, tip force, twisting angle, and power consumption. Based on the fabricated artificial fins, a small size and free swimming robotic manta ray has been developed. Experimental results show that the robot is able to swim at 0.055 BL/sec when the pectoral fins only flap.

There is still much opportunity to improve the robot speed. In the future work, we will improve the robot design in the following three aspects. First, a microcontroller based circuit board will be made to generate four channel control signals with tunable amplitude and phase. It will provide a platform for the robot to generate undulatory motions which will generate higher thrust force. Second, a more hydrodynamic robot body shape will be made to reduce the drag force. Third, a mathematic model for the robotic manta ray will be developed. It will help us to understand the propulsion mechanism of biological manta ray and provide useful information on how to optimize the design and control.

Acknowledgment

This research was supported in part by the Office of Naval Research (ONR) under the Multidisciplinary University Research Initiative (MURI) Grant N00014-08-1-0642 and the National Science Foundation (NSF) under the CAREER Grant CMS-0348448.

REFERENCES

1. "Manta rays." The Hawaii Association for Marine Education and Research, Inc., 2005.
2. L. J. Rosenberger, "Pectoral fin locomotion in batoid fishes: Undulation versus oscillation," *The Journal of Experimental Biology* **204**, pp. 379–394, 2001.
3. K. Moored, W. Smith, J. Hester, W. Chang, and H. Bart-Smith, "Investigating the thrust production of a myliobatoid-inspired oscillating wing," *Advances in Science and Technology* **58**, pp. 25–30, 2008.
4. K. Moored and H. Bart-Smith, "Investigation of clustered actuation in tensegrity structures," *International Journal of Solids and Structures* **46**, pp. 3272–3281, August 2009.
5. N. E. Leonard and J. G. Graver, "Model-based feedback control of autonomous underwater gliders," *IEEE Journal of Oceanic Engineering* **26**(4), pp. 633–645, 2001.
6. Y. Bar-Cohen, "Electroactive polymers as artificial muscles - capabilities, potentials and challenges," in *Handbook on Biomimetics*, Y. Osada, ed., pp. 1–13 (Chapter 8), NTS Inc., 2000.
7. M. Shahinpoor and K. Kim, "Ionic polymer-metal composites: I. Fundamentals," *Smart Materials and Structures* **10**, pp. 819–833, 2001.
8. K. J. Kim and M. Shahinpoor, "Ionic polymer-metal composites: II. manufaturing techniques," *Smart Materials and Structures* **12**, pp. 65–79, 2003.
9. Z. Chen and X. Tan, "A control-oriented and physics-based model for ionic polymer-metal composite actuators," *IEEE/ASME Transactions on Mechatronics* **13**(5), pp. 519–529, 2008.
10. Z. Chen and X. Tan, "Monolithic fabrication of ionic polymer-metal composite actuators capable of complex deformation," *Sensors and Actuators A: Physical* **157**(2), pp. 246–257, 2010.
11. M. Anton, A. Punning, A. Aabloo, M. Listak, and M. Kruusmaa, "Towards a biomimetic EAP robot," in *Proc. of Towards the Autonomous Mobile Robots*, pp. 1–7, 2004.
12. K. J. Kim and M. Shahinpoor, "A novel method of manufacturing three-dimensional ionic polymer-metal composites (IPMCs) biomimetic sensors, actuators, and artificial muscles," *Polymer* **43**, pp. 797–802, November 2002.
13. S. J. Kim, I. T. Lee, and Y. H. Kim, "Performance enhancement of IPMC actuator by plasma surface treatment," *Smart Materials and Structures* **16**, pp. N6–N11, January 2007.
14. C. Chung, P. Fung, Y. Hong, M. Ju, C. Lin, and T. Wu, "A novel fabrication of ionic polymer-metal composites (IPMC) actuator with silver nano-powders," *Sensors and Actuators B: Chemical* **117**, pp. 367–375, November 2006.
15. S. J. Lee, M. J. Han, S. JunKim, J. Jho, H. Y. Lee, and Y. H. Kim, "A new fabrication method for IPMC actuators and application to artificial fingers," *Smart Materials and Structures* **15**, pp. 1217–1224, August 2006.
16. S. Nemat-Nasser and J. Li, "Electromechanical response of ionic polymer-metal composites," *Journal of Applied Physics* **87**(7), pp. 3321–3331, 2000.
17. Z. Chen, S. Sharata, and X. Tan, "Modeling of biomimetic robotic fish propelled by an ionic polymer metal composite caudal fin," *IEEE/ASME Transactions on Mechatronics* **15**(3), pp. 448–459, 2010.
18. S. Shatara, X. Tan, E. Mbemmo, N. Gingery, and S. Henneberger, "Experimental investigation on underwater acoustic ranging for small robotic fish," in *Proceedings of the 2008 IEEE International Conference on Robotics and Automation*, pp. 712–717, (Pasadena, CA), 2008.